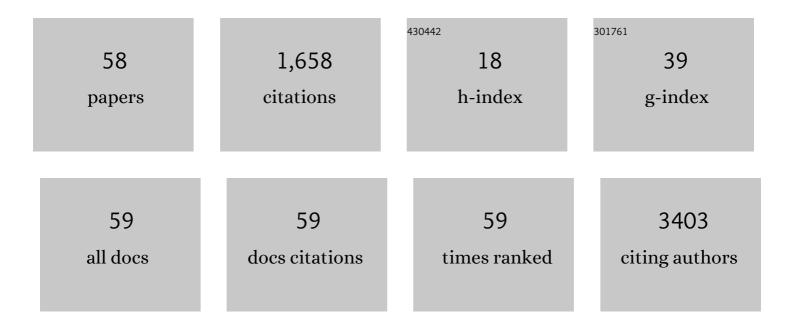
List of Publications by Year in descending order

Source: https://exaly.com/author-pdf/1909079/publications.pdf Version: 2024-02-01



Сні Мало

#	Article	IF	CITATIONS
1	EZH2 inhibition confers PIK3CA-driven lung tumors enhanced sensitivity to PI3K inhibition. Cancer Letters, 2022, 524, 151-160.	3.2	15
2	Mitochondrial superoxide targets energy metabolism to modulate epigenetic regulation of NRF2-mediated transcription. Free Radical Biology and Medicine, 2022, 179, 181-189.	1.3	4
3	A Review on Differential Abundance Analysis Methods for Mass Spectrometry-Based Metabolomic Data. Metabolites, 2022, 12, 305.	1.3	3
4	EBF1 promotes triple-negative breast cancer progression by surveillance of the HIF1α pathway. Proceedings of the National Academy of Sciences of the United States of America, 2022, 119, .	3.3	4
5	Genome-wide DNA methylation profiling in human breast tissue by Illumina TruSeq methyl capture EPIC sequencing and infinium methylationEPIC beadchip microarray. Epigenetics, 2021, 16, 754-769.	1.3	8
6	MEScan: a powerful statistical framework for genome-scale mutual exclusivity analysis of cancer mutations. Bioinformatics, 2021, 37, 1189-1197.	1.8	7
7	Gene expression barcode values reveal a potential link between Parkinson's disease and gastric cancer. Aging, 2021, 13, 6171-6181.	1.4	1
8	An ensemble of the iCluster method to analyze longitudinal lncRNA expression data for psoriasis patients. Human Genomics, 2021, 15, 23.	1.4	2
9	GEE-TGDR: A Longitudinal Feature Selection Algorithm and Its Application to IncRNA Expression Profiles for Psoriasis Patients Treated with Immune Therapies. BioMed Research International, 2021, 2021, 1-9.	0.9	1
10	Lapatinib and poziotinib overcome ABCB1-mediated paclitaxel resistance in ovarian cancer. PLoS ONE, 2021, 16, e0254205.	1.1	9
11	Cellular Origins of EGFRâ€Driven Lung Cancer Cells Determine Sensitivity to Therapy. Advanced Science, 2021, 8, e2101999.	5.6	13
12	Identification of long non-coding RNA signatures for squamous cell carcinomas and adenocarcinomas. Aging, 2021, 13, 2459-2479.	1.4	1
13	BRD4 modulates vulnerability of triple-negative breast cancer to targeting of integrin-dependent signaling pathways. Cellular Oncology (Dordrecht), 2020, 43, 1049-1066.	2.1	9
14	A Prognostic Model to Predict Recovery of COVID-19 Patients Based on Longitudinal Laboratory Findings. Virologica Sinica, 2020, 35, 811-819.	1.2	4
15	Identification of Monotonically Differentially Expressed Genes across Pathologic Stages for Cancers. Journal of Oncology, 2020, 2020, 1-9.	0.6	1
16	Combating acquired resistance to MAPK inhibitors in melanoma by targeting Abl1/2-mediated reactivation of MEK/ERK/MYC signaling. Nature Communications, 2020, 11, 5463.	5.8	24
17	Spermine synthase and MYC cooperate to maintain colorectal cancer cell survival by repressing Bim expression. Nature Communications, 2020, 11, 3243.	5.8	55
18	Improved workflow for mass spectrometry–based metabolomics analysis of the heart. Journal of Biological Chemistry, 2020, 295, 2676-2686.	1.6	26

#	Article	IF	CITATIONS
19	Differential Abundance Analysis with Bayes Shrinkage Estimation of Variance (DASEV) for Zero-Inflated Proteomic and Metabolomic Data. Scientific Reports, 2020, 10, 876.	1.6	2
20	The cox-filter method identifies respective subtype-specific lncRNA prognostic signatures for two human cancers. BMC Medical Genomics, 2020, 13, 18.	0.7	4
21	DACH1 mutation frequency in endometrial cancer is associated with high tumor mutation burden. PLoS ONE, 2020, 15, e0244558.	1.1	10
22	DACH1 mutation frequency in endometrial cancer is associated with high tumor mutation burden. , 2020, 15, e0244558.		0
23	DACH1 mutation frequency in endometrial cancer is associated with high tumor mutation burden. , 2020, 15, e0244558.		0
24	DACH1 mutation frequency in endometrial cancer is associated with high tumor mutation burden. , 2020, 15, e0244558.		0
25	DACH1 mutation frequency in endometrial cancer is associated with high tumor mutation burden. , 2020, 15, e0244558.		0
26	Predictive value of phenotypic signatures of bladder cancer response to cisplatin-based neoadjuvant chemotherapy. Urologic Oncology: Seminars and Original Investigations, 2019, 37, 572.e1-572.e11.	0.8	9
27	SDA: a semi-parametric differential abundance analysis method for metabolomics and proteomics data. BMC Bioinformatics, 2019, 20, 501.	1.2	4
28	Incorporating Pathway Information into Feature Selection towards Better Performed Gene Signatures. BioMed Research International, 2019, 2019, 1-12.	0.9	12
29	Feature Selection for Longitudinal Data by Using Sign Averages to Summarize Gene Expression Values over Time. BioMed Research International, 2019, 2019, 1-12.	0.9	3
30	Dose Reduction While Preserving Diagnostic Quality in Head CT: Advancing the Application of Iterative Reconstruction Using a Live Animal Model. American Journal of Neuroradiology, 2019, 40, 1864-1870.	1.2	1
31	A probabilistic method for leveraging functional annotations to enhance estimation of the temporal order of pathway mutations during carcinogenesis. BMC Bioinformatics, 2019, 20, 620.	1.2	0
32	Characterization of Squamous Cell Lung Cancers from Appalachian Kentucky. Cancer Epidemiology Biomarkers and Prevention, 2019, 28, 348-356.	1.1	5
33	Exosomal lipids for classifying early and late stage non-small cell lung cancer. Analytica Chimica Acta, 2018, 1037, 256-264.	2.6	72
34	A longitudinal feature selection method identifies relevant genes to distinguish complicated injury and uncomplicated injury over time. BMC Medical Informatics and Decision Making, 2018, 18, 115.	1.5	5
35	Targeting the BRD4/FOXO3a/CDK6 axis sensitizes AKT inhibition in luminal breast cancer. Nature Communications, 2018, 9, 5200.	5.8	71
36	To select relevant features for longitudinal gene expression data by extending a pathway analysis method. F1000Research, 2018, 7, 1166.	0.8	3

#	Article	IF	CITATIONS
37	Dub3 inhibition suppresses breast cancer invasion and metastasis by promoting Snail1 degradation. Nature Communications, 2017, 8, 14228.	5.8	101
38	ldentification of prognostic genes and gene sets for early-stage non-small cell lung cancer using bi-level selection methods. Scientific Reports, 2017, 7, 46164.	1.6	9
39	Snail determines the therapeutic response to mTOR kinase inhibitors by transcriptional repression of 4E-BP1. Nature Communications, 2017, 8, 2207.	5.8	27
40	Simultaneous quantitation of oxidized and reduced glutathione via LC-MS/MS: An insight into the redox state of hematopoietic stem cells. Free Radical Biology and Medicine, 2016, 97, 85-94.	1.3	24
41	NanoStringDiff: a novel statistical method for differential expression analysis based on NanoString nCounter data. Nucleic Acids Research, 2016, 44, gkw677.	6.5	100
42	Causal effect estimation in sequencing studies: a Bayesian method to account for confounder adjustment uncertainty. BMC Proceedings, 2016, 10, 411-415.	1.8	1
43	Weighted-SAMCSR: combining significance analysis of microarray-gene set reduction algorithm with pathway topology-based weights to select relevant genes. Biology Direct, 2016, 11, 50.	1.9	14
44	Elevated Glutathione Is Not Sufficient to Protect against Doxorubicin-Induced Nuclear Damage in Heart in Multidrug Resistance–Associated Protein 1 (Mrp1/Abcc1) Null Mice. Journal of Pharmacology and Experimental Therapeutics, 2015, 355, 272-279.	1.3	18
45	Accounting for uncertainty in confounder and effect modifier selection when estimating average causal effects in generalized linear models. Biometrics, 2015, 71, 654-665.	0.8	33
46	Test on existence of histology subtype-specific prognostic signatures among early stage lung adenocarcinoma and squamous cell carcinoma patients using a Cox-model based filter. Biology Direct, 2015, 10, 15.	1.9	25
47	A novel statistical method for quantitative comparison of multiple ChIP-seq datasets. Bioinformatics, 2015, 31, 1889-1896.	1.8	48
48	Loss of Multidrug Resistance–Associated Protein 1 Potentiates Chronic Doxorubicin-Induced Cardiac Dysfunction in Mice. Journal of Pharmacology and Experimental Therapeutics, 2015, 355, 280-287.	1.3	19
49	Novel Pharmacologic Targeting of Tight Junctions and Focal Adhesions in Prostate Cancer Cells. PLoS ONE, 2014, 9, e86238.	1.1	32
50	c-Abl and Arg induce cathepsin-mediated lysosomal degradation of the NM23-H1 metastasis suppressor in invasive cancer. Oncogene, 2014, 33, 4508-4520.	2.6	36
51	Multi-TGDR, a multi-class regularization method, identifies the metabolic profiles of hepatocellular carcinoma and cirrhosis infected with hepatitis B or hepatitis C virus. BMC Bioinformatics, 2014, 15, 97.	1.2	10
52	Disrupting the Interaction of BRD4 with Diacetylated Twist Suppresses Tumorigenesis in Basal-like Breast Cancer. Cancer Cell, 2014, 25, 210-225.	7.7	401
53	Autophagy Inhibition by Sustained Overproduction of IL6 Contributes to Arsenic Carcinogenesis. Cancer Research, 2014, 74, 3740-3752.	0.4	66
54	An Exponential Tilt Mixture Model for Time-to-Event Data to Evaluate Treatment Effect Heterogeneity in Randomized Clinical Trials. Biometrics & Biostatistics International Journal, 2014, 1, .	0.2	0

#	Article	IF	CITATIONS
55	A new shrinkage estimator for dispersion improves differential expression detection in RNA-seq data. Biostatistics, 2013, 14, 232-243.	0.9	210
56	Bayesian Effect Estimation Accounting for Adjustment Uncertainty. Biometrics, 2012, 68, 661-671.	0.8	84
57	Rejoinder: Bayesian Effect Estimation Accounting for Adjustment Uncertainty. Biometrics, 2012, 68, 680-686.	0.8	3
58	Exponential tilt models for two-group comparison with censored data. Journal of Statistical Planning and Inference, 2011, 141, 1102-1117.	0.4	9